

D3M: A DEEP DOMAIN DECOMPOSITION METHOD FOR PARTIAL DIFFERENTIAL EQUATIONS

KE LI¹*, KEJUN TANG¹*, TIANFAN WU[†], AND QIFENG LIAO^{*‡}

Abstract. A state-of-the-art deep domain decomposition method (D3M) based on the variational principle is proposed for partial differential equations (PDEs). The solution of PDEs can be formulated as the solution of a constrained optimization problem, and we design a multi-fidelity neural network framework to solve this optimization problem. Our contribution is to develop a systematical computational procedure for the underlying problem in parallel with domain decomposition. Our analysis shows that the D3M approximation solution converges to the exact solution of underlying PDEs. Our proposed framework establishes a foundation to use variational deep learning in large-scale engineering problems and designs. We present a general mathematical framework of D3M, validate its accuracy and demonstrate its efficiency with numerical experiments.

Key words. Domain decomposition, Deep learning, Mesh-free, Multi-fidelity, Parallel computation, PDEs, Physics-constrained

AMS subject classifications. 65M55, 68T05, 65N55

1. Introduction. Partial differential equations (PDEs) are among the most ubiquitous tools employed in describing computational science and engineering problems. When modeling complex problems, the governing PDEs are typically expensive to solve through transitional numerical methods, e.g., the finite element methods [9]. While principal component analysis [44, 35] (PCA), proper orthogonal decomposition [5, 43] (POD) and reduced basis methods [40, 31, 8, 6, 19, 13] are classical approaches for model reduction to reduce the computational costs, deep learning [16] currently gains a lot of interests for efficiently solving PDEs. There are mathematical guarantees called universal approximation theorems [12] stating that a single layer neural network can approximate most functions in Soblev spaces. Although there is still a lack of theoretical frameworks for explaining the effectiveness of multilayer neural networks, deep learning has become a widely used tool. Marvelous successful practices of deep neural networks encourages their applications to different areas, where the curse of dimensionality is a tormenting issue.

New approaches are actively proposed to solve PDEs based on deep learning techniques. E et al. [41, 42] connect deep learning with dynamic system and propose a deep Ritz method (DRM) for solving PDEs via variational methods. Raissi et al. [33, 34, 32] develop physics-informed neural networks which combine observed data with PDE models. By leveraging a prior knowledge that the underlying PDE model obeys a specific form, they can make accurate predictions with limited data. Long et al. [25] present a feed-forward neural network, called PDE-Net, to accomplish two tasks at the same time: predicting time-dependent behavior of an unknown PDE-governed dynamic system, and revealing the PDE model that generates observed data. Later, Sirignano et al. [37] propose a deep Galerkin method (DGM), which is a meshfree deep learning algorithm to solve PDEs without requiring observed data (solution samples of PDEs). When a steady-state high-dimensional parametric PDE system is considered, Zhu et al. [47, 48] propose Bayesian deep convolutional encoder-decoder networks for problems with high-dimensional random inputs.

When considering computational problems arising in practical engineering, e.g. aeronautics and astronautics, systems are typically designed by multiple groups along disciplinary. The complexity of solving large-scale problems may take an expensive cost of hardware. The balance of accuracy and generalization is also hard to trade off. For this reason, decomposing a given system into component parts to manage the complexity is a strategy, and the domain decomposition method is a traditional numerical method to achieve this goal. Schwarz [36] proposes an iterative method for solving harmonic functions. Then this method is improved by S.L.Sobolev [38], S.G.Michlin [27], P.L.Lions et al. [22, 23]. Domain decomposition is also employed for optimal design or control [2], for decomposing a complex design task (e.g., decomposition approaches to multidisciplinary optimization [21, 15]), and for uncertainty analysis of models governed by PDEs [20, 7].

In this work, we propose a variational deep learning solver based on domain decomposition methods, which is referred to as the deep domain decomposition method (D3M) to implement parallel computations along physical subdomains. Especially, efficient treatments of complex boundary conditions are developed. Solving PDEs using D3M has several benefits:

Complexity and generalization. D3M manages complexity at the local level. Overfitting is a challenging problem in deep learning. The risk of overfitting can be reduced by splitting the physical domain into subdomains, so that each network focuses on a specific subdomain.

^{*}School of Information Science and Technology, ShanghaiTech University, Shanghai, 200120, China. ¹ Equal contributions. ({like1, tangkj, liaoqf}@shanghaitech.edu.cn).

[†]Viterbi School of Engineering, University of Southern California, Los Angeles, USA, (tianfanw@usc.edu).

[‡]Corresponding author.

Mesh-free and data-free. D3M constructs and trains networks under variational formulation. So, it does not require given data, which can be potentially used for complex and high-dimensional problems.

Parallel computation. The computational procedures of D3M are in parallel for different subdomains. This feature helps D3M work efficiently on large-scale and multidisciplinary problems.

In this work, D3M is developed based on iterative domain decomposition methods. The development of using domain decomposition leads to an independent model-training procedure in each subdomain in an “offline” phase, followed by assembling global solution using pre-computed local information in an “online” phase. Section 2 reviews iterative overlapping domain decomposition methods. Section 3 presents the normal variational principle informed neural networks, and our D3M algorithms. A convergence analysis of D3M is discussed in Section 4, and a summary of our full approach is presented in Section 5. Numerical studies are discussed in Section 6. Finally, Section 7 concludes the paper.

2. Overlapping domain decomposition. The Schwarz method [36] is the most classical example of domain decomposition approach for PDEs, and it is still efficient with variant improvements [18, 45, 46].

Given a classical Poisson’s equation

$$(2.1) \quad \begin{cases} -\Delta u = f & , \text{ in } \Omega, \\ u = 0 & , \text{ on } \partial\Omega. \end{cases}$$

We divide Ω into two overlapping subdomains $\Omega_i, i = 1, 2$ (see Figure 2.1), where

$$(2.2) \quad \Omega = \Omega_1 \cup \Omega_2, \Gamma_1 := \partial\Omega_1 \cap \Omega_2, \Gamma_2 := \partial\Omega_2 \cap \Omega_1, \Omega_{1,2} := \Omega_1 \cap \Omega_2.$$

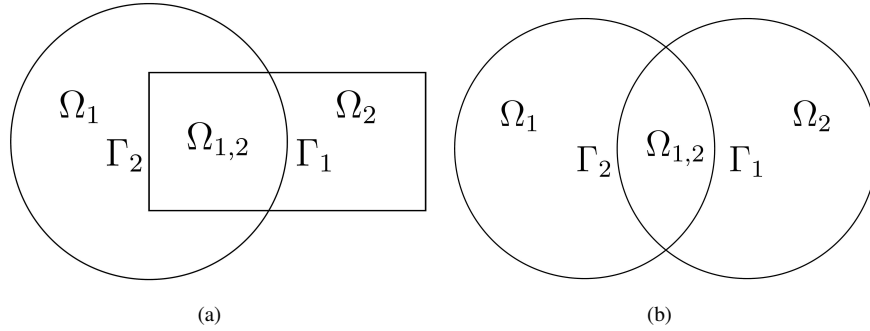


FIG. 2.1. Partition into two overlapping subdomains.

We introduce the original formula named Schwarz alternating method here. Let u^0 be an initial guess defined in Ω and vanishing on $\partial\Omega$. For $k \geq 0$, we define sequences u_i^k where u_i^k denotes u^k in Ω_i . The u_i^{k+1} is determined from an iteration algorithm:

$$(2.3) \quad \begin{cases} -\Delta u_1^{k+1/2} = f & , \text{ in } \Omega_1, \\ u_1^{k+1/2} = u_2^k & , \text{ on } \Gamma_1, \\ u_1^{k+1/2} = 0 & , \text{ on } \partial\Omega_1 \cap \partial\Omega \end{cases}$$

and

$$(2.4) \quad \begin{cases} -\Delta u_2^{k+1} = f & , \text{ in } \Omega_2, \\ u_2^{k+1} = u_1^{k+1/2} & , \text{ on } \Gamma_2, \\ u_2^{k+1} = 0 & , \text{ on } \partial\Omega_2 \cap \partial\Omega. \end{cases}$$

3. Deep domain decomposition method with variational principle. Before introducing D3M, we first give a brief introduction of variational principle. In this section, we consider the Poisson’s equation and reformulate (2.1) as a constrained minimization problem, and then we introduce the D3M algorithm.

3.1. Variational principle. The Poisson's equation with the homogeneous Dirichlet boundary condition is (2.1), and we consider the situation that $f \in \mathcal{L}^2(\Omega)$ and Ω is a square domain in this section. The idea of the standard Deep Ritz method is based on the variational principle. That is, the PDE can be derived by a functional minimization problem as described in the following proposition.

PROPOSITION 1. *Solving the Poisson's equation (2.1) is equivalent to an optimization problem*

$$(3.1) \quad \begin{aligned} \min_u E(u) &= \int_{\Omega} \frac{1}{2} |\nabla u|^2 dx dy - \int_{\Omega} f \cdot u dx dy, \\ \text{s.t. } u &= 0 \text{ on } \partial\Omega. \end{aligned}$$

The Lagrangian formula of (3.1) is given by

$$(3.2) \quad L(u, q) = \int_{\Omega} \frac{1}{2} |\nabla u|^2 dx dy - \int_{\Omega} u \cdot f dx dy + q \int_{\partial\Omega} u dx dy,$$

where q is the Lagrange multiplier.

DEFINITION 1. $\mathcal{H}(\mathbf{div})$ denotes symmetric tensor-fields in H^1 space, in which functions are square integrable and have square integrable divergence.

We employ a mixed residual loss [48] following Hellinger-Reissner principle [3]. With an additional variable $\tau \in \mathcal{H}(\mathbf{div})$, which represents flux, we can turn Equation (2.1) into

$$(3.3) \quad \begin{cases} \tau = -\nabla u & , \text{ in } \Omega, \\ \nabla \cdot \tau = f & , \text{ in } \Omega. \end{cases}$$

The mixed residual loss is

$$(3.4) \quad L(\tau, u, q) = \int_{\Omega} [(\tau + \nabla u)^2 + (\nabla \cdot \tau - f)^2] dx dy + q \int_{\partial\Omega} u dx dy.$$

3.2. Variational principle informed neural networks. Though the Poisson's equation (2.1) is reformulated as an optimization problem, it is intractable to find the optimum in an infinite-dimensional function space. Instead, we seek to approximate the solution $u(x, y)$ by neural networks. We utilize $N_u(x, y; \theta_u), N_{\tau}(x, y; \theta_{\tau})$ to approximate the solution u and the flux τ in domain Ω , where θ_u and θ_{τ} are the parameters to train. The input is the spatial variable in Ω , and the outputs represent the function value corresponding to the input. With these settings, we can train a neural network by variational principle to represent the solution of Poisson's equation. The functional minimization problem (3.4) turns into the following optimization problem

$$(3.5) \quad \min_{\theta=\{\theta_u, \theta_{\tau}\}} \int_{\Omega} [(N_{\tau} + \nabla N_u)^2 + (\nabla \cdot N_{\tau} - f)^2] dx dy + q \int_{\partial\Omega} N_u^2 dx dy.$$

REMARK 1. *In practical implementation, N_u and N_{τ} are embedded in one network N parameterized with θ , and the two outputs of N denote the function values of N_u and N_{τ} respectively.*

Therefore, the infinite-dimensional optimization problem (3.1) is transformed into a finite-dimensional optimization problem (3.5). Our goal is to find the optimal (or sub optimal) parameters θ to minimize the loss in (3.5). To this end, we choose a mini-batch of points randomly sampled in Ω . These data points can give an estimation of the integral in (3.5) and the gradient information to update the parameters θ . For example, a mini-batch points $\{(x_i, y_i)\}_{i=1}^{m+n}$ are drawn in $\bar{\Omega}$ randomly, where $\{(x_i, y_i)\}_{i=1}^m$ in Ω and $\{(x_i, y_i)\}_{i=1}^n$ on $\partial\Omega$. Then the parameters can be updated by using optimization approaches

$$(3.6) \quad \theta^{(k+1)} = \theta^{(k)} - \nabla_{\theta} \frac{1}{m} \sum_{i=1}^m [(N_{\tau}^{(i)} + \nabla N_u^{(i)})^2 + (\nabla \cdot N_{\tau}^{(i)} - f)^2] - \nabla_{\theta} \frac{1}{n} \sum_{j=1}^n (q \cdot N_u^{(j)})^2.$$

3.3. Implementation details for neural networks. This section provides details for the architecture of our neural networks.

For giving a direct-viewing impression, we show the implementation with a plain vanilla densely connected neural network to introduce how the structure works in Figure 3.1. For illustration only, the network depicted consists of 2

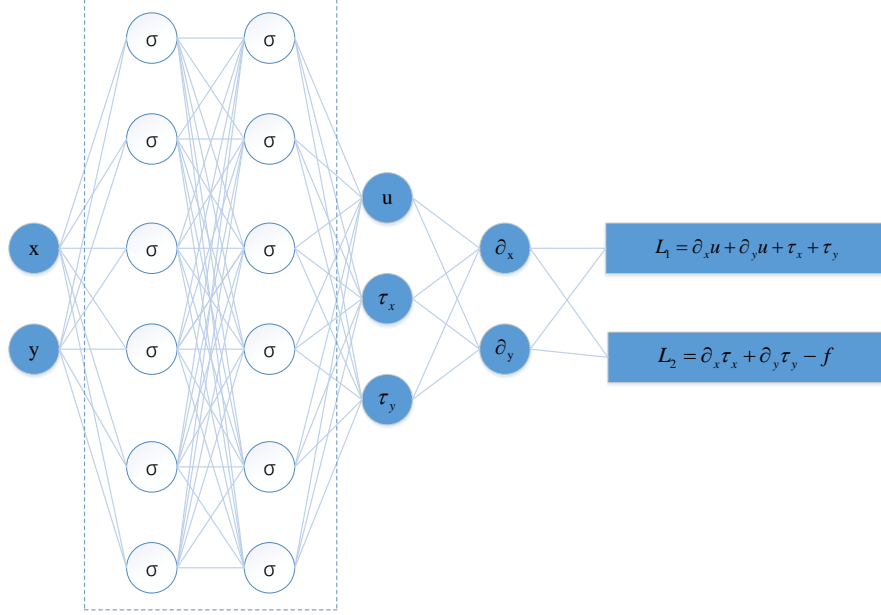


FIG. 3.1. Illustration of the neural networks. x, y are inputs, u, τ_x, τ_y are outputs and the dashed box with σ means the architecture of plain fully-connected neural networks.

layers with 6 neurons in each layer. The network takes input variables x, y and outputs $u, \tau = [\tau_x, \tau_y]$. The number of neurons in each layer is M and σ denotes an element-wise operator

$$(3.7) \quad \sigma(x) = (\phi(x_1), \phi(x_2), \dots, \phi(x_M)),$$

where ϕ is called the activation function. There are some commonly used activation functions such as the sigmoidal function, the tanh function, the rectified linear units (ReLU) function [28], and the Leaky ReLU function [26]. We employ the tanh function, and the automatic differentiation is obtained by using PyTorch [30]. The total loss function comprises the residual loss terms L_1, L_2 and the Lagrangian term which guarantees the constraint conditions. The parameters are trained with backpropogating gradients of the loss function and the optimizer is L-BFGS [24] where the learning rate is 0.5. In practice, the model architecture of neural networks is the residual network (ResNet) [11]. These residual networks are easier to optimize, and it can gain accuracy from considerably increased depth. The structure of ResNet improves the result of deep networks, because there are more previous information retained. A brief illustration of ResNet is in Figure 3.2.

3.4. Deep domain decomposition method. In this part, we propose the main algorithms of our D3M. Because the physics-constrained neural network is mesh-free, we improve Schwarz alternating method with a better inhomogeneous D3M sampling method at junctions Γ_i to accelerate convergence. We note the performance of normal deep variational networks and mixed residual networks can deteriorate when the underlying problem has inhomogeneous boundary conditions. Our treatment to overcome this weakness is to introduce the following boundary function.

DEFINITION 2. (Boundary function) A smooth function $g(x, y)$ is called a boundary function associated with Ω if

$$(3.8) \quad g(x, y) = e^{-a \cdot d(x, y, \partial\Omega)} u(x, y), \quad (x, y) \in \Omega,$$

where $a \gg 1$ is a coefficient, the notation $d(x, y, \partial\Omega)$ denotes the shortest Euclidean distance between (x, y) and $\partial\Omega$. If the point (x, y) is on the boundary, $g(x, y) = u(x, y)$. If not, the value of $g(x, y)$ decreases to zero sharply. And we define $v := u - g$, where v satisfies

$$(3.9) \quad \begin{cases} -\Delta v = f + \Delta g, & \text{in } \Omega, \\ v = 0, & \text{on } \partial\Omega. \end{cases}$$

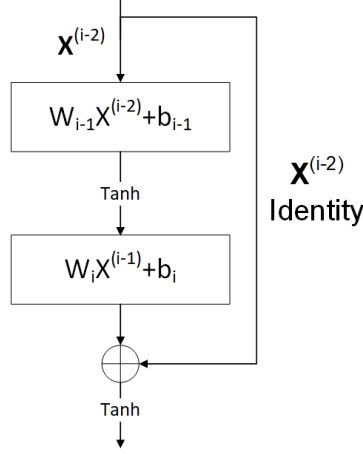


FIG. 3.2. The residual network building block of our method.

Letting $v_i = u_i - g_i$ on each subdomain, Equation (3.3) can be represented as

$$(3.10) \quad \begin{cases} \tau = -\nabla v_i, & \text{in } \Omega_i, \\ \nabla \cdot \tau = f + \Delta g_i, & \text{in } \Omega_i. \end{cases}$$

The mixed residual loss is

$$(3.11) \quad \begin{aligned} L(\tau_i, v_i, q) &= \int_{\Omega_i} [(\tau_i + \nabla v_i)^2 + (\nabla \cdot \tau_i - f - \Delta g_i)^2] dx dy + q \int_{\partial \Omega_i} v_i^2 dx dy, \\ &\approx \frac{1}{m_1} \sum_{k=1}^{m_1} [(\tau_i^{(k)} + \nabla v_i^{(k)})^2 + (\nabla \cdot \tau_i^{(k)} - f - \Delta g_i)^2] + \frac{1}{m_2} \sum_{j=1}^{m_2} q \cdot (v_i^{(j)})^2. \end{aligned}$$

It should be noted that, the integration is completed by Monte Carlo, such that the domain decomposition reduces the variance of samples significantly with the same number of data because the area of samples becomes smaller.

Algorithm 1 Deep domain decomposition

- 1: **Input:** $\Omega = (x_0, x_1) \times (y_0, y_1)$, p , Γ_i , η , θ , n , m_1 , m_2 .
 - 2: **Initialize:** $\epsilon = 10 \times \eta$, $k = 0$, $g v_i^0 = \mathbf{0}$, S_i , g_i .
 - 3: Divide the physical domain Ω into $\Omega_1, \dots, \Omega_p$.
 - 4: **while** $\epsilon > \eta$ **do**
 - 5: Run Algorithm (2) in each subdomain in parallel.
 - 6: $\epsilon = \frac{1}{p} \sum_{i=1}^p \|Sol_i^{(k+1)} - Sol_i^{(k)}\|_2^2$.
 - 7: $k = k + 1$.
 - 8: **end while**
 - 9: Merge p parts $Sol_i^{(k)}$ and get $Dnn_{sol}^{(k)}$.
 - 10: **Return:** $Dnn_{sol}^{(k)}$.
-

Algorithm 2 Training for subdomain Ω_i

- 1: **Input:** $S_i, gv_i^k, g_i^k, n, m_1, m_2$.
- 2: Construct function g_i using value of $gv_i^k, v_i = N_u - g_i$.
- 3: **for** n steps **do**
- 4: Sample minibatch of m_1 samples $\hat{S}_i = \{(x_i, y_i)\}_{i=1}^{m_1}$ in Ω_i .
- 5: Sample minibatch of m_2 samples $\hat{g}_i = \{(x_i, y_i)\}_{i=1}^{m_2}$ on $\partial\Omega_i$.
- 6: Update the parameters θ_i by descending its stochastic gradient:

$$\theta_i^{(k+1)} = \theta_i^{(k)} - \nabla_{\theta} \frac{1}{m_1} \sum_{k=1}^{m_1} [(N_{\tau}^{(k)} + \nabla v_i^{(k)})^2 + (\nabla \cdot N_{\tau}^{(k)} - f - \Delta g_i)^2] - \nabla_{\theta} \frac{1}{m_2} \sum_{j=1}^{m_2} (g \cdot v_i^{(j)})^2.$$

- 7: **end for**
- 8: $Sol_i^{(k+1)} = N_u(S_i)$.
- 9: $gv_i^{(k+1)} = N_u(g_i^{(k)})$.
- 10: **Return:** $Sol_i^{(k+1)}, gv_i^{(k+1)}$.

The procedure of D3M is as follows. We first divide the domain Ω into d subdomains, and each two neighboring subdomains are overlapping. The local solution of PDEs on each subdomain is replaced by neural networks which can be trained through the variational principle, where the global solution on the whole domain consists of these local solutions on subdomains. To be more precise, let Γ_i denote decomposed junctions, θ is initial weights of neural networks, η is the threshold of accuracy, S_i and g_i are the samples generated in Ω_i and on interface Γ_i to evaluate the output of networks in each iteration, \hat{S}_i are training samples in subdomain Ω_i , \hat{g}_i are training samples on Γ_i , n is training time in each iteration, m_1 and m_2 are batch sizes, N_u is the neural networks for u , N_{τ} is the neural networks for τ , k is the iteration time, and $Sol_i^{(k+1)}$ is the output of networks for subdomain Ω_i in $(k+1)$ -th iteration. The formal description of D3M is presented in Algorithm 1.

4. Analysis. While mixed residual formulation is a special case, we consider the basic functional formulation first,

$$(4.1) \quad J(u) = \int_{\Omega} \frac{1}{2} \nabla u \cdot \nabla u - f u dS.$$

DEFINITION 3. Given m closed subspaces $\{V_i\}_{i=1}^m$ and $V = \sum_{i=1}^m V_i \in C^2(\Omega)$, for any $R < \infty$, and a proper, lower semi-continuous, coercive convex functional $J : V \rightarrow \mathfrak{R}$, we denote $K_R := \{u \in V | J(u) < R\}$.

ASSUMPTION 1. $J \in C^1(K_R)$ and $\exists \alpha_R > 0$ s.t. $\forall v, u \in K_R$

$$(4.2) \quad J(v) - J(u) - (J'(u), v - u) \geq \alpha_R |v - u|^2,$$

where J' is uniformly continuous on K_R .

PROPOSITION 2. (P.L.Lions, 1989) The alternating Schwarz method (2.3) and (2.4) converges to the solution of u of Equation (3.10). The error bound of \hat{u}_1^{k+1} and \hat{u}_2^{k+1} can be estimated via maximum principle [14, 23], $\exists \rho \in (0, 1)$ such that for $\forall k \geq 0$

$$(4.3) \quad \|u|_{\Omega_i} - \hat{u}_i^{k+1}\|_{L^{\infty}(\Omega_i)} \leq \rho^k \|u|_{\Omega_i} - \hat{u}_i^0\|_{L^{\infty}(\Omega_i)},$$

where constants ρ is close to one if the overlapping region $\Omega_{i,j}$ is thin.

LEMMA 1. (K. Hornik, 1991) On each subdomain Ω_i , neural network N_i with continuous derivatives up to order K are universal approximators in Sobolev space with an order K , which means $N_i \in H^1(\Omega_i)$.

LEMMA 2. (P. L. Lions, 1988) If the variational formulation (4.1) satisfies the assumption (1), then it follows that there exists a sequential $u_n \in V_i$ obtained by Schwarz alternating method converges to the minimum u_i^* of $J(u_i)$ on each subdomain Ω_i .

THEOREM 1. $J_i(N_i)$ denotes the objective function on the subdomain Ω_i . Under above assumptions, for $\forall \epsilon > 0$, $\exists M > 0$, while iteration times $k > M$, N_i^k converges to optimal solution u_i^* of $J(u_i)$ in subdomain Ω_i for a constant $C > 0$

$$(4.4) \quad |N_i^k - u_i^*|^2 \leq C\epsilon^{1/2} \text{ in } \Omega_i.$$

For concision, we use N_i to represent N_i^k in the following part.

Proof. $u_n \in V_i$ denotes the sequential in Lemma 2, there exist

$$(4.5) \quad |u_n - u_i^*| \leq \frac{C_0}{\alpha_R} \omega |u_{n+1} - u_n|,$$

where $C_0 > 0$ is a constant, $\omega |u_{n+1} - u_n| = |J'(u_{n+1}) - J'(u_n)|$.

Then with Lemma 1 [12], in each subdomain Ω_i , neural network $N_i \in H^1$. If the training times k in each subdomain is enough, the universal approximation ensures the distance between functions N_i and u_n is close enough in the Sobolev space, with the constant $C_1 > 0$

$$(4.6) \quad |N_i - u_n|^2 \leq C_1^2 \epsilon^2.$$

While u_n converging to the minimum of u_i^* of $J(u)$, by the optimality conditions it is clear that

$$(4.7) \quad \begin{aligned} (J'(u_{n+1}), u_{n+1} - u_n) &< \epsilon, \\ (J'(u_{n+1}), u_{n+1} - u_i^*) &< \epsilon. \end{aligned}$$

Under the assumption, $\exists C > 0$ and the difference between two iterations can be represented as

$$(4.8) \quad |u_{n+1} - u_n|^2 \leq \frac{1}{\alpha_R} |J(u_{n+1}) - J(u_n)| \leq \frac{1}{\alpha_R} \epsilon$$

Consider equation (4.5), (4.6) and (4.8), we have

$$(4.9) \quad \begin{aligned} |N_i - u_i^*| &\leq |N_i - u_n| + |u_n - u_i^*|, \\ &\leq C_1 \epsilon + \frac{C_0}{\alpha_R} \omega |u_{n+1} - u_n|, \\ &\leq C \epsilon^{1/2}. \end{aligned}$$

□

THEOREM 2. For a given boundary function g and a fixed q , the optimal solution N_u^* of Equation (3.5) and v^* of Equation (3.10) satisfy $N_u^* = v^* + g$.

Proof. We use τ and ϕ to denote $-\nabla N_u$ and $-\nabla v$ respectively.

$$(4.10) \quad \begin{aligned} L(\phi, v) &= \int_{\Omega} [(\phi + \nabla v)^2 + (\nabla \cdot \phi - f - \Delta g)^2] dx dy + q \int_{\partial\Omega} v dx dy, \quad \text{if } v|_{\partial\Omega} = 0 \\ &= \int_{\Omega} [(\tau + \nabla g + \nabla u - \nabla g)^2 + (\nabla \cdot \tau - f)^2] dx dy + q \int_{\partial\Omega} (u - g) dx dy \\ &= L(\tau, u). \end{aligned}$$

Function v we optimized is also the optimal solution N_u with the formula $N_u^* = v^* + g$. □

Up to now, we prove that D3M can solve steady Poisson's equation with variational formulations. Then, we extend D3M to more general quasilinear parabolic PDEs (4.11) with physics-constrained approaches.

$$(4.11) \quad \begin{cases} \operatorname{div}(\alpha(x, u_i(x), \tau_i(x))) + \gamma(x, u_i(x), \tau_i(t, x)) = 0, & x \in \Omega_i \\ u_i(t, x) = 0, & x \in \partial\Omega_i \end{cases}$$

where τ_i denotes ∇u_i , and $\Omega_i \in \mathbb{R}^d$ are decomposed boundary sets with smooth boundaries $\partial\Omega_i$. We recall the network space of subdomain Ω_i with generated data according to [12]

$$(4.12) \quad \mathfrak{N}_i^n(\sigma) = \left\{ h(x) : \mathbb{R}^k \rightarrow \mathbb{R} \mid h(x) = \sum_{j=1}^n \beta_j \sigma(\alpha_j^T x - \theta_j) \right\}$$

where σ is any activation function, $\mathbf{x} \in \mathbb{R}^k$ is one set of generated data, $\beta \in \mathbb{R}^n$, $\alpha \in \mathbb{R}^{k \times n}$ and $\theta \in \mathbb{R}^{k \times n}$ denote coefficients of networks. Set $\mathfrak{N}_i(\sigma) = \bigcup_{i=1}^{\infty} \mathfrak{N}_i^n(\sigma)$. Under the universal approximation of neural networks Lemma 1, in each subdomain the neural networks f_i^n satisfies

$$(4.13) \quad \begin{cases} \operatorname{div}(\alpha(x, f_i^n(x), \tau_i^n(x))) + \gamma(x, f_i^n(x), \tau_i^n(t, x)) = h^n, & x \in \Omega_i \\ f_i^n(t, x) = b^n, & x \in \partial\Omega_i \end{cases}$$

where h^n and b^n satisfy

$$(4.14) \quad \|h^n\|_{2,\Omega_i}^2 + \|b^n\|_{2,\partial\Omega_i}^2 \rightarrow 0, \text{ as } n \rightarrow \infty.$$

For the following part of analysis, we make some assumptions.

ASSUMPTION 2.

- There is a constant $\mu > 0$ and positive functions $\kappa(x), \lambda(x)$ such that for all $x \in \Omega_i$ we have

$$\|\alpha(x, u_i, \tau_i)\| \leq \mu(\kappa(x) + \|\tau_i\|),$$

and

$$|\gamma(x, u_i, \tau_i)| \leq \lambda(x)\|\tau_i\|,$$

with $\kappa \in L^2(\Omega_i), \lambda \in L^{d+2+\eta}(\Omega_i)$ for some $\eta > 0$.

- $\alpha(x, u_i, \nabla u_i)$ and $\gamma(x, u_i, \nabla u_i)$ are Lipschitz continuous in $(x, u_i, \nabla u_i) \in \Omega \times \mathbb{R} \times \mathbb{R}^d$.
- In each subdomain, the derivatives of solutions from alternating Schwarz method (2.3), (2.4) converge to the derivative of solution u_i . Precisely, there exists a constant $\rho_1 \in (0, 1)$, such that for iteration times $\forall k \geq 0$

$$\|\nabla u_i^* - \nabla u_i^k\|_\infty \leq \rho_1 \|\nabla u_i^* - \nabla u_i^0\|_\infty.$$

- $\alpha(x, u, \tau)$ is continuously differentiable w.r.t. (t, x) .
- There is a positive constant $\nu > 0$ such that

$$\alpha(x, u, \tau)\tau \geq \nu|\tau|^2$$

and $\forall \tau_1, \tau_2 \in \mathbb{R}^d, \tau_1 \neq \tau_2$

$$\langle \alpha(x, u, \tau_1) - \alpha(x, u, \tau_2), \tau_1 - \tau_2 \rangle > 0.$$

THEOREM 3. Suppose the domain Ω is decomposed into $\{\Omega_i\}_{i=1}^p$, $k > 0$ denotes iteration times (omitted in notations for brief). $\mathfrak{N}_i(\psi)$ denotes networks space space in subdomain Ω_i , where subdomains are compact. Assume that target function (4.11) has unique solution in each subdomain, nonlinear terms $\text{div}(x, u, \nabla u)$ and $\gamma(x, u, \nabla u)$ are locally Lipschitz in $(u_i, \nabla u_i)$, and ∇u_i^k uniformly converges to ∇u_i^* with k . For $\forall \epsilon > 0$, there $\exists K > 0$ such that there exists a set of neural networks $\{N_i \in \mathfrak{N}_i(\psi)\}_{i=1}^p$ satisfies the L^2 error $E_2(N_i)$ as follow

$$(4.15) \quad \sum_{i=1}^p \lim_{k \rightarrow \infty} E_2(N_i) \leq K\epsilon.$$

Proof. In each subdomain Ω_i , with iteration times $k > 0$, $E_2^k(N_i)$ denotes the L^2 loss between N_i^k and u_i^* .

$$(4.16) \quad \begin{aligned} \lim_{k \rightarrow \infty} E_2^k(N_i) &= \|\text{div}(\alpha(x, u_i^*(x), \nabla u_i^*(x))) + \gamma(x, u_i^*(x), \nabla u_i^*(x)) \\ &\quad - [\text{div}(\alpha(x, N_i(x), \nabla N_i(x))) + \gamma(x, N_i(x), \nabla N_i(x))]\|_{\Omega_i}^2 + \|N_i\|_{\partial\Omega_i}^2 \end{aligned}$$

With Lemma 1, it is clear that the sum of last term is smaller than $K_1\epsilon$, where $K_1 > 0$ is a constant. We assumed that ∇u_i^k uniformly converges to ∇u_i^* with k , and this means that

$$(4.17) \quad \|\nabla u_i^* - \nabla u_i^k\|_\infty \leq \rho_1 \|\nabla u_i^* - \nabla u_i^0\|_\infty.$$

So that we have

$$(4.18) \quad \begin{aligned} \lim_{k \rightarrow \infty} E_2^k(N_i) &\leq \int_{\Omega_i} |\text{div}(\alpha(x, u_i^*(x), \nabla u_i^*(x))) - \text{div}(\alpha(x, u_i^k(x), \nabla u_i^k(x))) + \text{div}(\alpha(x, u_i^k(x), \nabla u_i^k(x))) - \text{div}(\alpha(x, N_i(x), \nabla N_i(x)))| dx \\ &\quad + \int_{\Omega_i} |\gamma(x, u_i^*(x), \nabla u_i^*(x)) - \gamma(x, u_i^k(x), \nabla u_i^k(x)) + \gamma(x, u_i^k(x), \nabla u_i^k(x)) - \gamma(x, N_i(x), \nabla N_i(x))| dx + K_1\epsilon \\ &\leq \int_{\Omega_i} |\text{div}(\alpha(x, u_i^*(x), \nabla u_i^*(x))) - \text{div}(\alpha(x, u_i^k(x), \nabla u_i^k(x)))| dx + \int_{\Omega_i} |\text{div}(\alpha(x, u_i^k(x), \nabla u_i^k(x))) - \text{div}(\alpha(x, N_i(x), \nabla N_i(x)))| dx \\ &\quad + \int_{\Omega_i} |\gamma(x, u_i^*(x), \nabla u_i^*(x)) - \gamma(x, u_i^k(x), \nabla u_i^k(x))| dx + \int_{\Omega_i} |\gamma(x, u_i^k(x), \nabla u_i^k(x)) - \gamma(x, N_i(x), \nabla N_i(x))| dx + K_1\epsilon \\ &\leq \int_{\Omega_i} |\text{div}(\alpha(x, u_i^*(x), \nabla u_i^*(x))) - \text{div}(\alpha(x, u_i^k(x), \nabla u_i^k(x)))| dx + \int_{\Omega_i} |\gamma(x, u_i^*(x), \nabla u_i^*(x)) - \gamma(x, u_i^k(x), \nabla u_i^k(x))| dx + K_2\epsilon + K_1\epsilon \end{aligned}$$

where $K_2 > 0$ is a constant, and the error bound between u_i^k and N_i^k is proved from Theorem 7.1 in [37].

(4.19)

$$\begin{aligned}
& \lim_{k \rightarrow \infty} \int_{\Omega_i} |\operatorname{div}(\alpha(x, u_i^*(x), \nabla u_i^*(x))) - \operatorname{div}(\alpha(x, u_i^k(x), \nabla u_i^k(x)))|^2 dx \\
& \leq \int_{\Omega_i} (|u_i^k|^{q_1} + |\nabla u_i^k|)^{q_2} + |u_i^*|^{q_3} + |\nabla u_i^*|^{q_4} \times (|u_i^* - u_i^k| + |\nabla u_i^* - \nabla u_i^k|) dx \\
& \leq \left(\int_{\Omega_i} (|u_i^k - u_i^*|^{q_1} + |\nabla u_i^k - \nabla u_i^*|^{q_2} + |u_i^*|^{\max\{q_1, q_3\}} + |\nabla u_i^*|^{\max\{q_2, q_4\}}) dx \right)^{1/r} \times \left(\int_{\Omega_i} \rho^k \|u_i^* - u_i^0\|_\infty + \rho_1^k \|\nabla u_i^* - \nabla u_i^0\|_\infty dx \right) \\
& \leq \left(\int_{\Omega_i} \|u_i^k - u_i^*\|_\infty^{q_1} + \|\nabla u_i^k - \nabla u_i^*\|_\infty^{q_2} + \sup_{\Omega_i} |u_i^*|^{\max\{q_1, q_3\}} + \sup_{\Omega_i} |\nabla u_i^*|^{\max\{q_2, q_4\}} dx \right) \epsilon \\
& \leq K_3 \epsilon
\end{aligned}$$

where $K_3 > 0$ is a constant depends on ϵ . While $\gamma(\cdot)$ is also Lipschitz continuous, we can prove the upper bound of $\int_{\Omega_i} |\gamma(x, u_i^*(x), \nabla u_i^*(x)) - \gamma(x, u_i^k(x), \nabla u_i^k(x))| dx$ in the same formula with Equation (4.19), denoted as $K_4 \epsilon$. Hence we can obtain

$$(4.20) \quad \sum_{i=1}^P \lim_{k \rightarrow \infty} E_2(N_i) \leq \sum_{i=1}^P (K_1 \epsilon + K_2 \epsilon + K_3 \epsilon + K_4 \epsilon) \leq K \epsilon$$

□

THEOREM 4. *Under Assumption 2 and Equation (4.14), with iteration times $k \rightarrow \infty$, the set of neural networks N_i converge to the unique solutions to (4.11), strongly in $\mathcal{L}^p(\Omega_i)$ for every $p < 2$. In addition, in each subdomain the sequence $\{N_i^n(x)\}_{n \in \mathbb{N}}$ is bounded in n under the constraint of Proposition 2 and converges to u_i .*

Proof. In each subdomain, the convergence can be obtained from the Theorems 7.1 and 7.3 in [37]. With the Proposition 2, the sequence $\{N_i^n\}_{n \in \mathbb{N}}$ is uniform bounded in n , and the rates of convergence to the solution u^* are related to overlapping areas. □

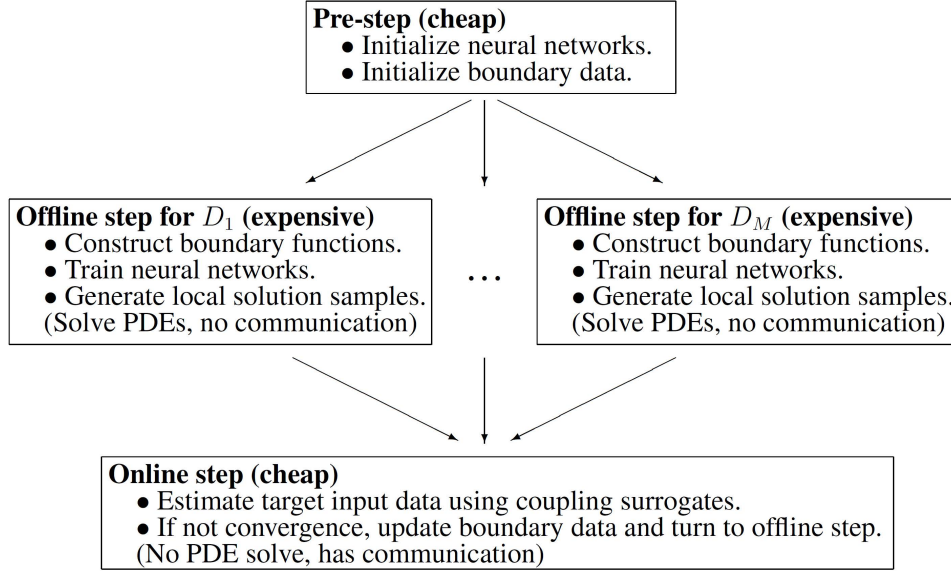
Specially, the n in $\{N_i^n(x)\}_{n \in \mathbb{N}}$ means training times instead of iteration times. We leave the proof for time-dependent data-free variational formulations for future work.

5. D3M summary. To summarize the strategies in Section 3 and 4, the full procedure of D3M comprises the following steps:

- pre-step: Set the architecture of neural networks in each subdomain;
- offline step: Construct functions for boundary conditions, train networks and generate local solutions;
- online step: Estimate target input data using neural networks. If solutions don't converge, transfer information on interfaces and go back to the offline step.

The pre-step is cheap, because the setting of neural networks is an easy task. In the offline stage, the complex system is fully decomposed into component parts, which means that there is no data exchange between subdomains. Since we only approximate the data on interface with normal simple approach such as Fourier series and polynomial chaos [7, 4], the approximation is also low costly. After decomposition, the requirement for number of samples for the Monte Carlo integration of the residual loss function (3.11) is significantly reduced, while the density of samples does not change. Since the number of samples decreasing and the domain becoming simpler, we can use neural networks with few layers to achieve a relatively high accuracy. If we keep the same number of samples and layers as the global setting, D3M should obtain a better accuracy. The cost of the online step is low, since no PDE solve is required. This full approach is also summarized in Figure 5.1, where transformations of data happen between adjacent subdomains.

For the problems we focus on (systems governed by PDEs), the cost of the D3M is dominated by the local training procedures in the offline step. Here we present a rough order of magnitude analysis of the computational costs where C_{solve} denotes the cost of one block in each training epoch (i.e., the cost of any block with the same number of neurons in each training iteration is taken to be equal for simplicity). The dominant cost of D3M is the total number of blocks of neural network and training times, $\sum_{i=1}^P N_i B_i T_i C_{\text{solve}}$, where N_i is sample size, B_i is number of blocks and T_i is training times. If we consider equal offline sample sizes, number of blocks and training epochs, $N_i = N_{\text{off}}, B_i = B_{\text{off}}, T_i = T_{\text{off}}$ for all subdomains $\{D_i\}_{i=1}^P$, then total cost can be written as $p N_{\text{off}} B_{\text{off}} T_{\text{off}} C_{\text{solve}}$. The total cost is decreased by employing the idea of hierarchical neural networks [29, 17].

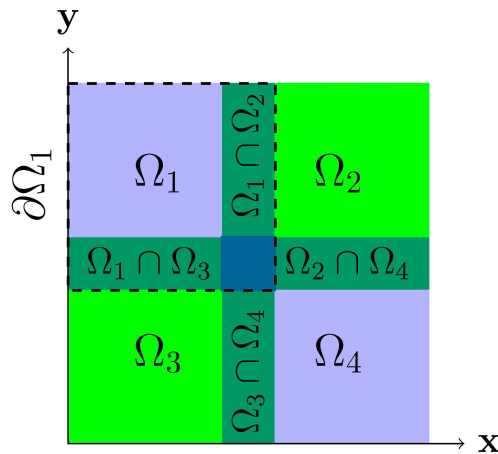
Fig. 5.1. *D3M summary.*

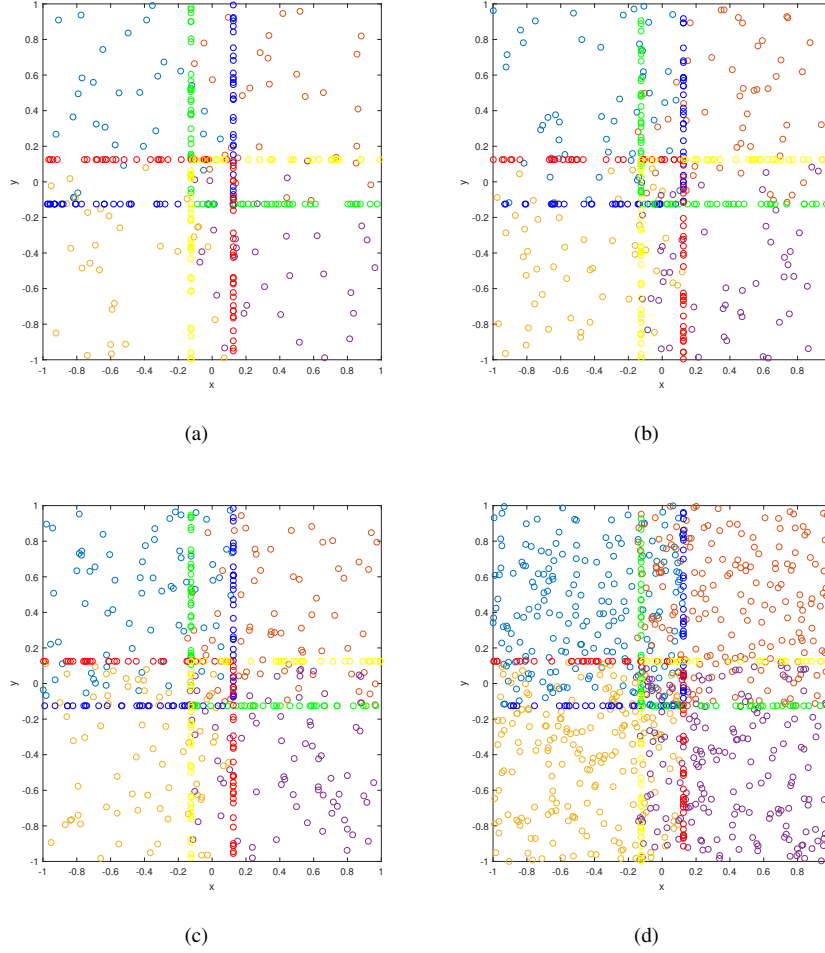
6. Numerical tests. Here we consider two classical problems, the Poisson's equation and the time-independent Schrödinger equation, to verify the performance of our D3M. All timings conduct on an Intel Core i5-7500, 16GB RAM, Nvidia GTX 1080Ti processor with PyTorch 1.0.1 [30] under Python 3.6.5. We train the networks only 30 epoch using L-BFGS in numerical tests (cost within two minutes).

6.1. Poisson's equation.

$$(6.1) \quad \begin{cases} -\Delta u(x, y) = 1, & \text{in } \Omega, \\ u(x, y) = 0, & \text{on } \partial\Omega, \end{cases}$$

where the physical domain is $\Omega = (-1, 1) \times (-1, 1)$. The domain decomposition setting is illustrated in Figure 6.1. To further improve the efficiency of D3M, we propose a new type of sampling methods. We randomly sample in each subdomain, and the number of samples increases with iteration times increase. The sample size on interfaces remains the same to provide an accurate solution for data exchange. An illustration of our D3M sampling method is represented in Figure 6.2

Fig. 6.1. *Illustrations of the physical domain with four overlapping components.*

FIG. 6.2. *D3M sampling : a new type of mesh-free sampling.*

REMARK 2. According to the research on overfitting, the hypothesis set (w.r.t. the complexity of neural networks) should match the quantity and quality of data instead of target functions [1]. So in the initial several iterations, the number of residual blocks is small. The number increases while the sample size in Figure 6.2 increases.

After decomposition, with designed g_i satisfying Definition 1 for each subdomains, the function $v_i := u_i - g_i$ satisfies the homogeneous Poisson's equation and follows (2.3) and (2.4).

The results of D3M is shown in 6.3(a). For comparison, we plot the result of normal deep Ritz method (DRM) with the same type of network and the finite element method (FEM) in Figure 6.3(b) and 6.3(c). We set the result of FEM as the groundtruth and define the relative error $e_r = \frac{\|sol - fem_{sol}\|_2}{\|fem_{sol}\|_2}$. We compare results using residual network (ResNet), and the comparison including relative errors are shown in Table 6.1. We can see that with the same setting for networks, our D3M offers a higher accuracy than normal DRM in this experiment.

TABLE 6.1
The relative error for Poisson's equation.

Method	Net type	Blocks	Number of neurons	Relative error
DRM	ResNet	4	2048	0.0271
DRM	ResNet	8	4096	0.0157
D3M	ResNet	4	2048	0.0065
D3M	ResNet	8	4096	0.0045

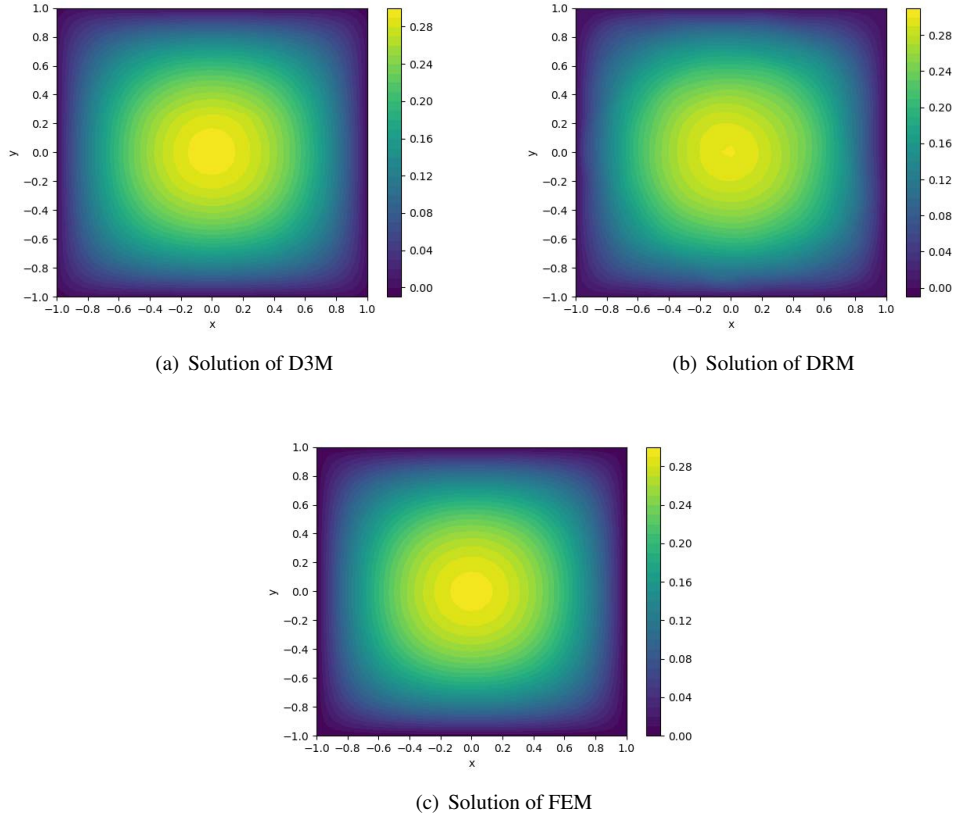


FIG. 6.3. Solutions computed by three different methods.

6.2. Schrödinger equation. In the area of domain decomposition methods, the steady-state Schrödinger equation is one of the classical problems [39, 10].

$$(6.2) \quad \left[\frac{-\hbar^2}{2m} \nabla^2 + V(\mathbf{r}) \right] \Psi(\mathbf{r}) = E\Psi(\mathbf{r}).$$

Where $\hbar = \frac{h}{2\pi}$ is the reduced Planck constant, m is the particle's mass and E is a known constant related to the energy level. This equation occurs often in quantum mechanics where $V(\mathbf{r})$ is the function for potential energy. Here we consider an infinite potential well

$$(6.3) \quad V(\mathbf{r}) = \begin{cases} 0, & \mathbf{r} \in [0, 1]^d \\ \infty, & \mathbf{r} \notin [0, 1]^d. \end{cases}$$

The variational loss is

$$(6.4) \quad \begin{aligned} L(\tau_i, N_i, q) &= \int_{\Omega_i} [\Delta N_i(r) + \Delta g_i - EN_i(r) + Eg_i] dr \\ &+ q \int_{\partial\Omega_i} (N_i(r))^2 dr + \gamma \left(\int_{\Omega_i} |N_i(r)|^2 dr - 1 + P_i \right)^2, \end{aligned}$$

where $\int_{\Omega} |\Psi(r)|^2 dr = 1$, because $\Psi(r)$ is the wave function and $\Psi(r)^2$ means the probability density of particle appearing. P_i denotes the probability of particle appearing in $\Omega \setminus \Omega_i$. It should be noted that N_i is an approximation of $\Psi(r)_i - g_i$, where $\Psi(r)_i$ is the global solution $\Psi(r)$ restricted on the subdomain Ω_i and g_i is the boundary function for the interface of Ω_i .

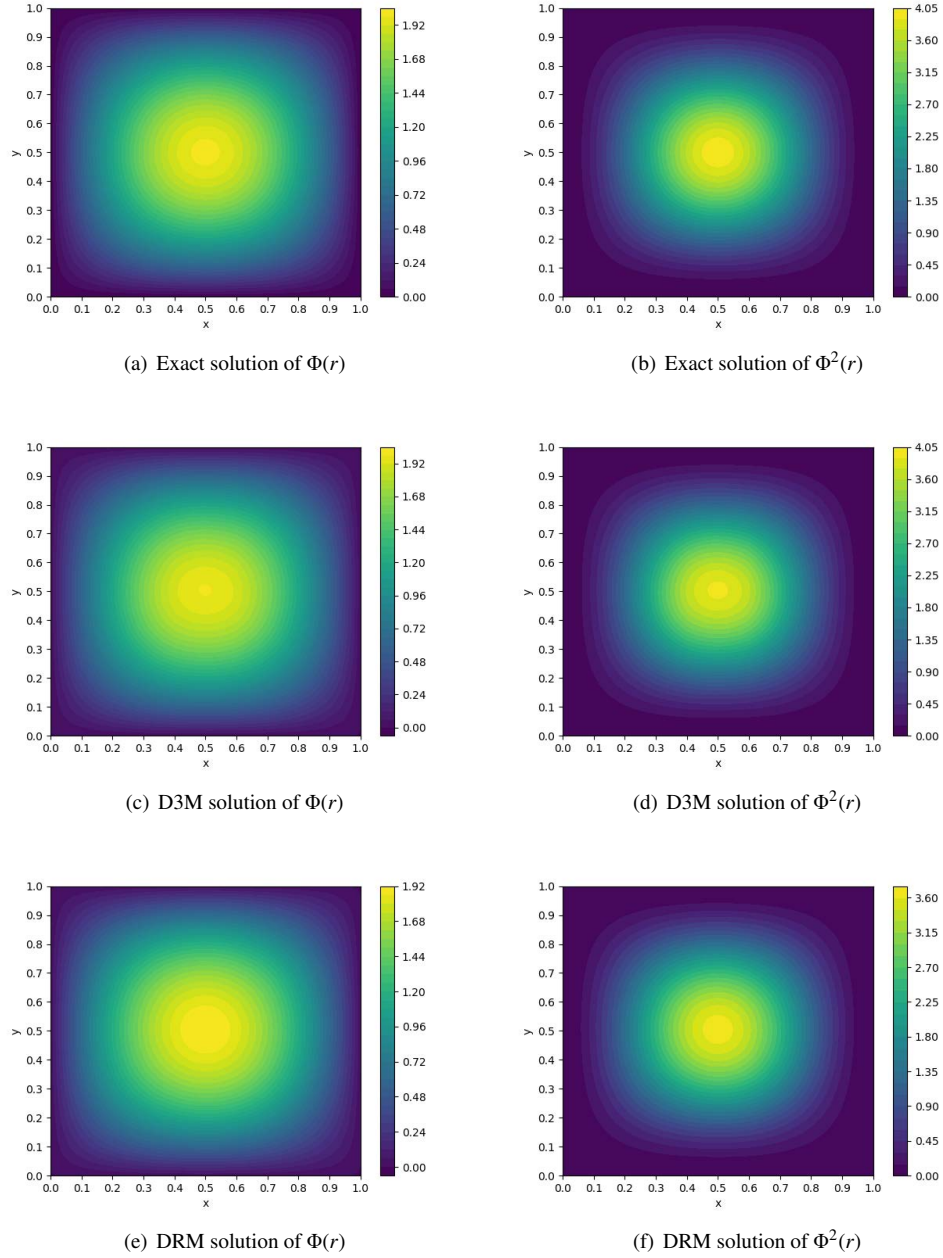


FIG. 6.4. The solutions of wave function and probability density for a time-independent Schrödinger equation.

For this two dimensional time-independent Schrödinger equation, we can calculate the analytical solution $\Psi(r) = A \sin(\frac{m\pi r_1}{b})C \sin(\frac{n\pi r_2}{a})$, where $A = C = \sqrt{2}$, $a = b = 1$ and $n = m = 1$ in this infinite potential well case with domain $[0, 1] \times [0, 1]$. As shown in Figure 6.4, excellent agreement can be achieved between the exact solutions and predictions from our D3M. Compared with the solutions of DRM, D3M shows a better performance especially in peak values. The comparison of accuracy for both the wave equation and the probability density is shown in Table 6.2 and Figure 6.5. Under the same conditions including network structure, Lagrangian multiplier, learning rate, number of samples and training epoch, our D3M shows smaller errors in both wave equation and probability density.

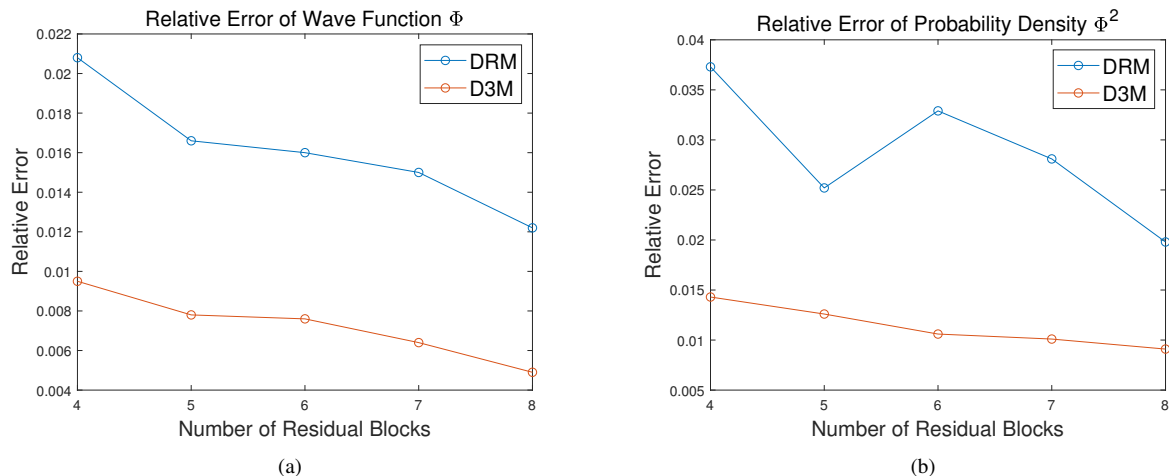


FIG. 6.5. Comparison of relative errors corresponding to different number of residual blocks.

TABLE 6.2
Relative errors for the wave function and the probability density.

Target	Method	Net type	Blocks	Number of neurons	Relative error
Wave	DRM	ResNet	4	2048	0.0209
Wave	DRM	ResNet	8	4096	0.0169
Wave	D3M	ResNet	4	2048	0.0095
Wave	D3M	ResNet	8	4096	0.0045
Prob.	DRM	ResNet	4	2048	0.0357
Prob.	DRM	ResNet	8	4096	0.0334
Prob.	D3M	ResNet	4	2048	0.0143
Prob.	D3M	ResNet	8	4096	0.0091

7. Conclusion. This paper has proposed a new deep domain decomposition method. The most significant contribution of the proposed approach is parallel computation, which lays a foundation for employing physics-constrained deep learning framework in large-scalar engineering simulations or designs. This is accomplished by incorporating domain decomposition method into the loss function. Based on the property of mesh-free, we propose a new D3M sampling method to improve computational efficiency. And our framework absorbs the idea of mixed finite element method, so that the boundary condition can be satisfied more accurately. We have demonstrated that deep domain decomposition method can solve general parabolic PDEs with high accuracy. Furthermore, the generalization performance of D3M should be better, because domains are smaller.

In theory, our approach is feasible to solve complex systems with many subdomains and corresponding neural networks. In practice, the approach suffers from three main bottlenecks. One is that a bad initialization of neural networks can lead to superfluous cost for following iterations. One is the choice of function for approximating interfaces. And another is that the choice of Lagrangian multiplier is important but lacks of prior. We leave these questions for future work.

Acknowledgments. This work is supported by the National Natural Science Foundation of China (No. 11601329).

REFERENCES

- [1] Y. S. ABU-MOSTAFA, M. MAGDON-ISMAIL, AND H.-T. LIN, *Learning from data*, vol. 4, AMLBook New York, NY, USA:, 2012.
- [2] H. ANTIL, M. HEINKENSCHLOSS, R. H. HOPPE, AND D. C. SORENSEN, *Domain decomposition and model reduction for the numerical solution of pde constrained optimization problems with localized optimization variables*, *Computing and Visualization in Science*, 13 (2010), pp. 249–264.
- [3] D. N. ARNOLD, *Mixed finite element methods for elliptic problems*, *Computer Methods in Applied Mechanics and Engineering*, 82 (1990), pp. 281 – 300. *Proceedings of the Workshop on Reliability in Computational Mechanics*.

- [4] M. ARNST, R. GHANEM, E. PHIPPS, AND J. RED-HORSE, *Dimension reduction in stochastic modeling of coupled problems*, International Journal for Numerical Methods in Engineering, 92 (2012), pp. 940–968.
- [5] G. BERKOOZ, P. HOLMES, AND J. L. LUMLEY, *The proper orthogonal decomposition in the analysis of turbulent flows*, Annual review of fluid mechanics, 25 (1993), pp. 539–575.
- [6] P. CHEN, A. QUARTERONI, AND G. ROZZA, *Comparison between reduced basis and stochastic collocation methods for elliptic problems*, Journal of Scientific Computing, 59 (2014), pp. 187–216.
- [7] Y. CHEN, J. JAKEMAN, C. GITTELSON, AND D. XIU, *Local polynomial chaos expansion for linear differential equations with high dimensional random inputs*, SIAM Journal on Scientific Computing, 37 (2015), pp. A79–A102.
- [8] H. C. ELMAN AND Q. LIAO, *Reduced basis collocation methods for partial differential equations with random coefficients*, SIAM/ASA Journal on Uncertainty Quantification, 1 (2013), pp. 192–217.
- [9] H. C. ELMAN, D. J. SILVESTER, AND A. J. WATHEN, *Finite elements and fast iterative solvers: with applications in incompressible fluid dynamics*, Oxford University Press (UK), 2014.
- [10] T. HAGSTROM, R. P. TEWARSON, AND A. JAZCILEVICH, *Numerical experiments on a domain decomposition algorithm for nonlinear elliptic boundary value problems*, Applied Mathematics Letters, 1 (1988), pp. 299–302.
- [11] K. HE, X. ZHANG, S. REN, AND J. SUN, *Deep residual learning for image recognition*, in Proceedings of the IEEE conference on computer vision and pattern recognition, 2016, pp. 770–778.
- [12] K. HORNIK, *Approximation capabilities of multilayer feedforward networks*, Neural networks, 4 (1991), pp. 251–257.
- [13] J. JIANG, Y. CHEN, AND A. NARAYAN, *A goal-oriented reduced basis methods-accelerated generalized polynomial chaos algorithm*, SIAM/ASA Journal on Uncertainty Quantification, 4 (2016), pp. 1398–1420.
- [14] L. KANTOROVICH AND V. KRYLOV, *Approximate methods of higher analysis*, Bull Amer Math Soc, 66 (1960), pp. 146–147.
- [15] F. KONG, V. KHEYFETS, E. FINOL, AND X.-C. CAI, *An efficient parallel simulation of unsteady blood flows in patient-specific pulmonary artery*, International journal for numerical methods in biomedical engineering, 34 (2018), p. e2952.
- [16] Y. LECUN, Y. BENGIO, AND G. HINTON, *Deep learning*, nature, 521 (2015), p. 436.
- [17] K. LI, K. TANG, J. LI, T. WU, AND Q. LIAO, *A hierarchical neural hybrid method for failure probability estimation*, IEEE Access (in press), (2019).
- [18] S. LI, X. SHAO, AND X.-C. CAI, *Multilevel space-time additive schwarz methods for parabolic equations*, SIAM Journal on Scientific Computing, 40 (2018), pp. A3012–A3037.
- [19] Q. LIAO AND G. LIN, *Reduced basis anova methods for partial differential equations with high-dimensional random inputs*, Journal of Computational Physics, 317 (2016), pp. 148–164.
- [20] Q. LIAO AND K. WILLCOX, *A domain decomposition approach for uncertainty analysis*, SIAM Journal on Scientific Computing, 37 (2015), pp. A103–A133.
- [21] Z.-J. LIAO, R. CHEN, Z. YAN, AND X.-C. CAI, *A parallel implicit domain decomposition algorithm for the large eddy simulation of incompressible turbulent flows on 3d unstructured meshes*, International Journal for Numerical Methods in Fluids, 89 (2019), pp. 343–361.
- [22] P.-L. LIONS, *On the schwarz alternating method. i*, in First international symposium on domain decomposition methods for partial differential equations, vol. 1, Paris, France, 1988, p. 42.
- [23] ———, *On the schwarz alternating method ii*, Domain decomposition methods, 628 (1989), pp. 47–70.
- [24] D. C. LIU AND J. NOCEDAL, *On the limited memory bfgs method for large scale optimization*, Mathematical programming, 45 (1989), pp. 503–528.
- [25] Z. LONG, Y. LU, X. MA, AND B. DONG, *PDE-net: Learning pdes from data*, arXiv preprint arXiv:1710.09668, (2017).
- [26] A. L. MAAS, A. Y. HANNUN, AND A. Y. NG, *Rectifier nonlinearities improve neural network acoustic models*, in Proc. icml, vol. 30, 2013, p. 3.
- [27] S. MIKHLIN, *On the schwarz algorithm*, in Dokl. Akad. Nauk SSSR, vol. 77, 1951, pp. 569–571.
- [28] V. NAIR AND G. E. HINTON, *Rectified linear units improve restricted boltzmann machines*, in Proceedings of the 27th international conference on machine learning (ICML-10), 2010, pp. 807–814.
- [29] L. W. NG AND K. E. WILLCOX, *Multifidelity approaches for optimization under uncertainty*, International Journal for numerical methods in Engineering, 100 (2014), pp. 746–772.
- [30] A. PASZKE, S. GROSS, S. CHINTALA, G. CHANAN, E. YANG, Z. DEVITO, Z. LIN, A. DESMAISON, L. ANTIGA, AND A. LERER, *Automatic differentiation in pytorch*, (2017).
- [31] A. QUARTERONI AND G. ROZZA, *Numerical solution of parametrized Navier-Stokes equations by reduced basis methods*, Numerical Methods for Partial Differential Equations, 23 (2007), pp. 923–948.
- [32] M. RAISSI, P. PERDIKARIS, AND G. KARNIADAKIS, *Physics-informed neural networks: A deep learning framework for solving forward and inverse problems involving nonlinear partial differential equations*, Journal of Computational Physics, 378 (2019), pp. 686–707.
- [33] M. RAISSI, P. PERDIKARIS, AND G. E. KARNIADAKIS, *Physics informed deep learning (part i): Data-driven solutions of nonlinear partial differential equations*, arXiv preprint arXiv:1711.10561, (2017).
- [34] ———, *Physics informed deep learning (part ii): Data-driven discovery of nonlinear partial differential equations*, arXiv preprint arXiv:1711.10566, (2017).
- [35] B. SCHÖLKOPF, A. SMOLA, AND K.-R. MÜLLER, *Kernel principal component analysis*, in International conference on artificial neural networks, Springer, 1997, pp. 583–588.
- [36] H. A. SCHWARZ, *Ueber einen Grenzübergang durch alternirendes Verfahren*, Zürcher u. Furrer, 1870.
- [37] J. SIRIGNANO AND K. SPILIOPOULOS, *DGM: A deep learning algorithm for solving partial differential equations*, Journal of Computational Physics, 375 (2018), pp. 1339–1364.
- [38] S. SOBOLEV, *The schwarz algorithm in the theory of elasticity*, in Dokl. Acad. Nauk., USSR, vol. 2, 1936, pp. 235–238.
- [39] A. TOSELLI AND O. WIDLUND, *Domain decomposition methods-algorithms and theory*, vol. 34, Springer Science & Business Media, 2006.
- [40] K. VEROY, D. ROVAS, AND A. PATERA, *A posteriori error estimation for reduced-basis approximation of parametrized elliptic coercive partial differential equations: “Convex Inverse” bound conditioners*, ESAIM: Control, Optimisation and Calculus of Variations, 8 (2002), pp. 1007–1028.
- [41] E. WEINAN, *A proposal on machine learning via dynamical systems*, Communications in Mathematics and Statistics, 5 (2017), pp. 1–11.
- [42] E. WEINAN AND B. YU, *The deep ritz method: A deep learning-based numerical algorithm for solving variational problems*, Communications in Mathematics and Statistics, 6 (2018), pp. 1–12.

- [43] K. WILLCOX AND J. PERAIRE, *Balanced model reduction via the proper orthogonal decomposition*, AIAA journal, 40 (2002), pp. 2323–2330.
- [44] S. WOLD, K. ESSENSEN, AND P. GELADI, *Principal component analysis*, Chemometrics and intelligent laboratory systems, 2 (1987), pp. 37–52.
- [45] S. ZAMPINI AND X. TU, *Multilevel balancing domain decomposition by constraints deluxe algorithms with adaptive coarse spaces for flow in porous media*, SIAM Journal on Scientific Computing, 39 (2017), pp. A1389–A1415.
- [46] D. ZHANG, L. YANG, AND G. E. KARNIADAKIS, *Bi-directional coupling between a pde-domain and an adjacent data-domain equipped with multi-fidelity sensors*, Journal of Computational Physics, 374 (2018), pp. 121–134.
- [47] Y. ZHU AND N. ZABARAS, *Bayesian deep convolutional encoder–decoder networks for surrogate modeling and uncertainty quantification*, Journal of Computational Physics, 366 (2018), pp. 415–447.
- [48] Y. ZHU, N. ZABARAS, P.-S. KOUTSOURELAKIS, AND P. PERDIKARIS, *Physics-constrained deep learning for high-dimensional surrogate modeling and uncertainty quantification without labeled data*, Journal of Computational Physics, 394 (2019), pp. 56–81.